Manufacturing Technologies and Applications MATECA



Experimental and Numerical Investigation of Wear Behavior of Monel 400 Alloy under Different Load and Speed Conditions

Mehmet Tayyip Özdemir^{1,*} , Mustafa Buğday¹

¹Department of Mechanical Engineering, Engineering Faculty, Karabük University, Karabük, Türkiye

ABSTRACT

In this study, the wear behavior of Monel 400 alloy under different load and speed conditions was investigated using both experimental tests and numerical simulations. Wear tests were carried out using tungsten carbide (WC) ball with high hardness and abrasiveness. In the experiments, it was observed that there was a significant increase in the wear rate with the increase in applied load and speed. It was determined that especially at high loads, the material loss on the surface accelerated and more distinct wear marks were formed on the contact surface. The simulations performed were modeled based on Archard's wear law and verified with the experimental data obtained. According to the results obtained by simulation, the stress on the abrasive ball surface increases as speed and force increase. A maximum error rate of 12.30% was calculated between the simulation results and the experimental data, which shows that the finite element model is quite reliable in wear predictions. For example, in the wear tests carried out at a speed of 50 mm/s, a 168.4% increase in material volume loss occurred when the load was increased from 30 N to 50 N. This finding reveals the significant effect of the load on wear mechanisms. The studies show that the developed finite element model is successful in calculating wear deformations. In addition, results supporting that Monel 400 is a material with high wear resistance and can be used in applications requiring wear resistance in particular have been obtained. Future studies can be expanded to include different abrasive materials, changing environmental conditions and more complex loading scenarios.

Keywords: Tribology, Wear, Friction, Volume loss

Monel 400 Alaşımının Farklı Yük ve Hız Koşulları Altında Aşınma Davranışının Deneysel ve Savısal İncelenmesi

ÖZET

Bu çalışmada, Monel 400 alaşımının farklı yük ve hız koşulları altındaki aşınma davranışı hem deneysel testler hem de sayısal simülasyonlar kullanılarak incelenmiştir. Aşınma testleri, sertliği ve aşındırıcılığı yüksek olan tungsten karbür (WC) bilyesi kullanılarak gerçekleştirilmiştir. Deneylerde, uygulanan yük ve hızın artmasıyla aşınma miktarında belirgin bir yükselme olduğu gözlenmiştir. Özellikle yüksek yüklerde, yüzeydeki malzeme kaybının hızlandığı ve temas yüzeyinde daha belirgin aşınma izlerinin oluştuğu tespit edilmiştir. Gerçekleştirilen simülasyonlar, Archard'ın aşınma yasasına dayalı olarak modellenmiş ve elde edilen deneysel verilerle doğrulanmıştır. Simülasyonla elde edilen sonuçlara göre aşındırıcı top yüzeyinde meydana gelen gerilme hız ve kuvvet arttıkça artmaktadır. Simülasyon sonuçları ile deneysel veriler arasında maksimum %12,30 hata oranı hesaplanmıştır ki bu, sonlu elemanlar modelinin aşınma tahminlerinde oldukça güvenilir olduğunu göstermektedir. Örneğin, 50 mm/s hızda yapılan aşınma testlerinde, yük 30 N'dan 50 N'a çıkarıldığında malzeme hacim kaybında %168,4'lük bir artış meydana gelmiştir. Bu bulgu, yükün aşınma mekanizmaları üzerindeki önemli etkisini ortaya koymaktadır. Yapılan çalışmalar, geliştirilen sonlu elemanlar modelinin aşınma deformasyonlarını hesaplamada başarılı olduğunu göstermektedir. Ayrıca, Monel 400'ün yüksek aşınma direncine sahip bir malzeme olduğunu ve özellikle aşınma direnci gerektiren uygulamalarda kullanılabileceğini destekleyen sonuçlar elde edilmiştir. Gelecekte yapılacak çalışmalar, farklı aşındırıcı malzemeler, değişen çevresel koşullar ve daha karmaşık yükleme senaryolarını içerecek şekilde genişletilebilir.

Anahtar Kelimeler: Triboloji, Aşınma, Sürtünme, Hacim kaybı

1. INTRODUCTION

Monel 400 is a special alloy based on nickel and copper and is widely used in industrial applications with its outstanding corrosion resistance, mechanical strength and thermal stability [1,2]. Its resistance to high temperatures and harsh operating conditions makes it a preferred material in critical areas such as nuclear reactors, chemical process equipment, aviation and marine applications [3,4]. However, despite these

^{*}Corresponding author, e-mail: tayyipozdemir@karabuk.edu.tr

properties, alloys such as Monel 400 can face certain challenges from wear mechanisms. Wear can cause surface deterioration in metal materials, reducing their functional life and increasing maintenance costs [5,6]. Therefore, identifying different wear mechanisms in Monel 400 and understanding the wear behavior of this material is critical to optimizing its industrial use. Due to the high wear risk of Monel alloys, the tribological distribution of this material has been the subject of research for many years. Today, researchers focus on studying the wear of Monel 400 under different conditions. Esgin et al. investigated the wear properties of different Monel alloys produced by powder metallurgy and determined the highest mass consumption properties of Monel 400 under the same test conditions. In addition, only the wear ranges of this alloy were determined during the wear test [1]. Ma et al. investigated the tribocorrosion behavior of Monel 400 by abrasion and wear tests under different loads in an artificial seawater environment. Regardless of the load amount, small and scattered areas were observed on the surface after the wear test and it was concluded that abrasion is the pressing mechanism in the tribocorrosion process of abrasion [7]. Kukliński et al. investigated wear resistance and reported that microstructural alterations in Monel 400, resulting from processes like laser boriding, could enhance its hardness and, consequently, its wear properties. Their study primarily examined microhardness, concluding that optimised laser treatments could enhance the wear resistance properties of this alloy [2,8]. Furthermore, research on cavitation erosion and erosive wear indicates that the mechanical properties and wear resistance of Monel 400 are considerably influenced by its microstructure, underscoring the importance of composition and processing conditions in determining wear performance [9]. Furthermore, the challenges related to the processing of Monel 400 hinder its use in manufacturing environments, as evidenced by multiple machining studies. Research has been conducted on Electrical Discharge Machining (EDM) techniques to optimise the manufacturing of components from Monel 400. Modifications in EDM parameters, including pulse duration and current, significantly influence material removal rates and tool wear during machining. These factors are essential for preserving the integrity of the alloy throughout the machining process [10-12]. Kukliński et al. examined the potential of advanced surface treatment techniques, specifically laser alloying, to improve the wear resistance and mechanical performance of Monel 400 under extreme operating conditions through boron coating [8,13].

Research has examined the impact of surface modification and material composition on wear resistance. Findings indicate that the boring process enhances wear performance, while load and speed are critical factors influencing abrasive wear. Additionally, BN-MXene reinforcements have been found to enhance the dry sliding wear behaviour of AA7075 alloy [14].

Wear studies on different composite materials and metals and Finite element method (FEM) simulations are among the widely researched topics in the field of tribology. The pin-disc test setup is one of the basic experimental methods widely used in wear analysis. FEM based software such as ANSYS and ABAQUS are preferred for numerical analysis. The first modeling study to predict wear behavior was developed by Archard [15], and this model was applied to different types of wear and was found to be in good agreement with experimental wear data.

Firaol et al. [16] conducted a detailed study on wear measurement and wear analysis of overhead line contact wire using ANSYS Workbench software. Sullivan developed a mathematical model that describes the relationship between applied load and wear, and various factors were considered as Archard wear coefficient in this model [17]. The authors conducted experimental studies including finite element analysis of sliding wear in metals. The model was formulated in Lagrangian framework and Archard law was used in wear calculations. Validation of the model was carried out using a brass pin rotating on a steel disk [18].

This study covers experimental studies and numerical simulation analyses to investigate the wear behavior of Monel 400 alloy. The samples for the wear test were prepared following G133 standards, and the test was conducted using a flat ball tester. Furthermore, experiments were conducted at loads of 30 N, 40 N, and 50 N, with speeds of 40 mm/s and 50 mm/s over 100 meters. In the experimental section, wear experiments will be carried out on Monel 400 samples under various test conditions and the volume loss and friction coefficient of the material will be investigated. Additionally, numerical simulations performed in ANSYS Ls-Dyna software using the finite element method (FEM) were used to predict the wear behavior of Monel 400 and the results were compared with experimental data. In this way, the study will provide a comprehensive approach to better understand the wear mechanisms in Monel 400 with both experimental and numerical methods. Determining the wear mechanisms in Monel 400 is a critical step to increase the longevity and performance of this material. The findings obtained by combining experimental and numerical analyses can guide engineering applications in design and material selection. In this context, the results of the study are expected to make significant contributions to industrial areas that utilize Monel 400, especially in heavy-duty conditions.

2. MATERIAL AND METHOD

2.1. Dry Sliding Wear Simulation

Wear behavior was investigated in ANSYS package program using FEM approach. Wear depths agree with the experiment. The methodology used in the analysis is presented in the following sections.

2.2. Modeling Geometry

The geometry model was created by ANSYS design modeler. The ball and plate FE model was given a perfect contact constraint. The diameter of the abrasive ball (WC) is 6 mm, the abrasive plate (Monel 400) is 5 mm high, 6 mm wide and 2 mm thick. Ansys package program uses Archard's wear model to simulate wear. The FE model is meshed according to a minimum size as shown in Figure 1. The plate has a quadrilateral mesh, while the mesh pattern on the ball is triangular and quadrilateral.

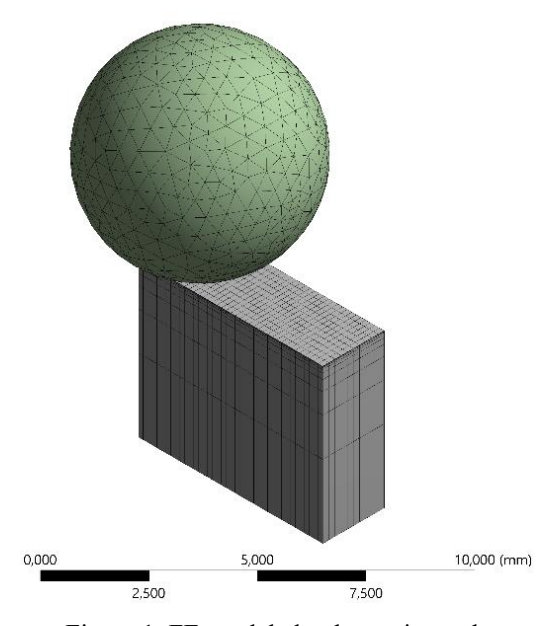


Figure 1. FE-modeled volumetric mesh.

2.3. Experimental Wear Test

Monel 400 material was used in this test. Its chemical composition is given in Table 1.

Table 1. Chemical composition of Monel 400 material.

Material	Ni	Fe	С	Mn	Si	S	Cu
Monel 400	%63	%2,5	%0,30	%2	%0,5	%0,024	%28

The surface of the samples to be subjected to abrasion testing was first sanded with 800 grit sandpaper and then with 1200 grit sandpaper. Then, it was polished with 3 µm Al₂O₃ suspension. After preparing the samples to be subjected to abrasion testing, a ball on flat test device was used in accordance with ASTM G133 standards [19–21]. Ball on flat wear device is in Karabuk University Mechanical Engineering Tribology Laboratory. The wear device has a maximum speed of 60 mm/s and a maximum stroke length of 30 mm. In this study, the stroke length was determined as 10 mm [22]. WC was used as the abrasive ball [22–24]. Additionally, tests were carried out under 30 N, 40 N and 50 N loads, at 40 mm/s and 50 mm/s speeds and at a distance of 100 meters. The chosen loads, speeds, and distances for the wear test were established through a comprehensive analysis of existing literature, industry standards, and preliminary experiments, ensuring they accurately reflect the operational conditions commonly experienced in real-world applications of Monel 400, thereby yielding reliable and pertinent results [25,26]. Additionally, each experiment was repeated 3 times, and the averages of the results were used. During the experiments, the friction coefficient value is obtained instantly from the wear test device. The concept of the friction coefficient can be described as the ratio of the frictional force to the normal load acting between two contacting surfaces. It is essential to note that the friction coefficient is not a static value; it varies with conditions such as surface roughness, material properties, and lubrication [27].

3. EXPERIMENT AND OPTIMIZATION RESULTS

The wear behavior of friction samples was tested by finite element and experimental methods. Experimental data and simulation results are presented in this section by extrapolating according to the principles of Archard's wear law [15].

3.1. Evaluation of Stresses on Abrasive Ball in Simulation

The abrasive ball was kept in contact with the wear surface by making a linear movement throughout the test. Pure sliding is observed between the ball and the plate during the test. The plate material moved equally under each load examined. Figure 2 shows the Von-misses stress contours on the abrasive ball from the simulation performed at variable loads and speeds. In order to reduce the calculation time, the analyses were performed at one stroke length. According to the results obtained by simulation, the lowest stress on the abrasive ball surface occurred at a speed of 40 mm/s and a load of 30 N, while the highest stress occurred at a speed of 50 mm/s and a load of 50 N.

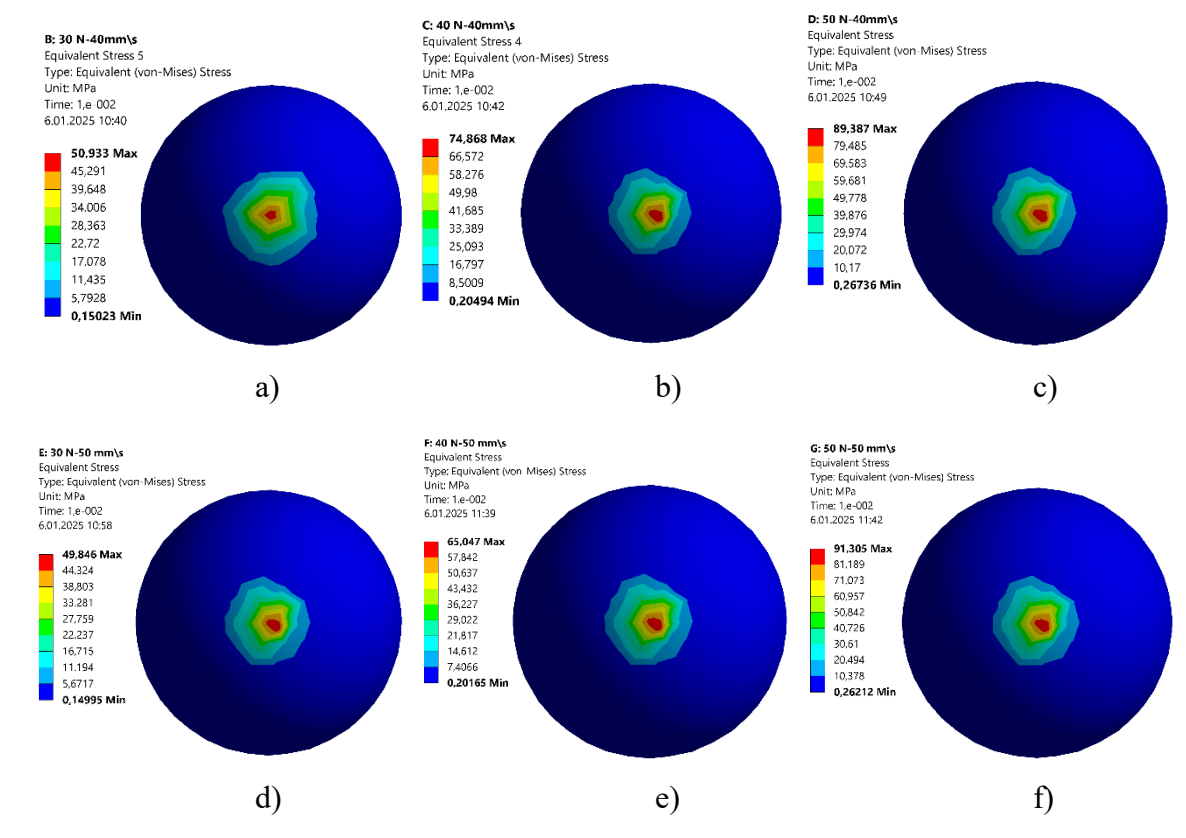


Figure 1. Von-Mises stress distribution on the abrasive ball 40 mm/s a) 30 N b) 40 N c) 50 N; 50 mm/s d) 30 N e) 40 N f) 50 N.

In Figure 2, as the test load increased, the Von-Mises stress value on the ball increased. At a wear rate of 40 mm/s (Figure 2a, b, and c), the stress value is 50.933 MPa and 89.387 MPa under loads of 30 N and 50 N, respectively. At a wear rate of 50 mm/s (Figure 2d, e, and f), the stress values on the ball are 49.846 MPa and 91.305 MPa, respectively. At 40 mm/s, the stress value increased by 75% (Figure 2a to Figure 2c) and at 50 mm/s, it increased by 83% (Figure 2d to Figure 2f). In Figure 3, the stress region on the ball is within an average diameter of 4 mm for all test results.

3.2. Evaluation of Volume Loss in Wear

The amount of deformation on the worn surface was calculated by averaging the data taken from three lines in the simulation. In the experimental study, the wear depth was determined by averaging the data taken from three regions with a profilometer. Then, the volume losses were calculated. The volume loss values obtained in the experimental and simulation studies are compared in Figure 3. In the simulation, the wear values of these materials were determined without taking into account the so-called third layer or friction layer that forms at the interface between the plate and the ball during the sliding of the friction material. This friction layer on the ball surface acts as a lubricant, providing load-bearing capability and serving as a buffer zone, which helps

reduce the wear rate of the contacting materials. When the agreement between the simulation and experimental studies is examined in Figure 4, the average deviation in the studies conducted at 40 mm/s speed is obtained as 6.17%. The average deviation at 50 mm/s speed is obtained as 12.30%. The average volume loss value obtained in the studies conducted at 40 mm/s speed is 0.0426 mm³. The average volume loss value obtained at 50 mm/s speed has increased by 17.91% compared to 40 mm/s speed. When the results are examined in general, the study conducted by Çakır [28] and Odabas [29] supports these results. In these studies, as the speed increases, the volume loss increases.

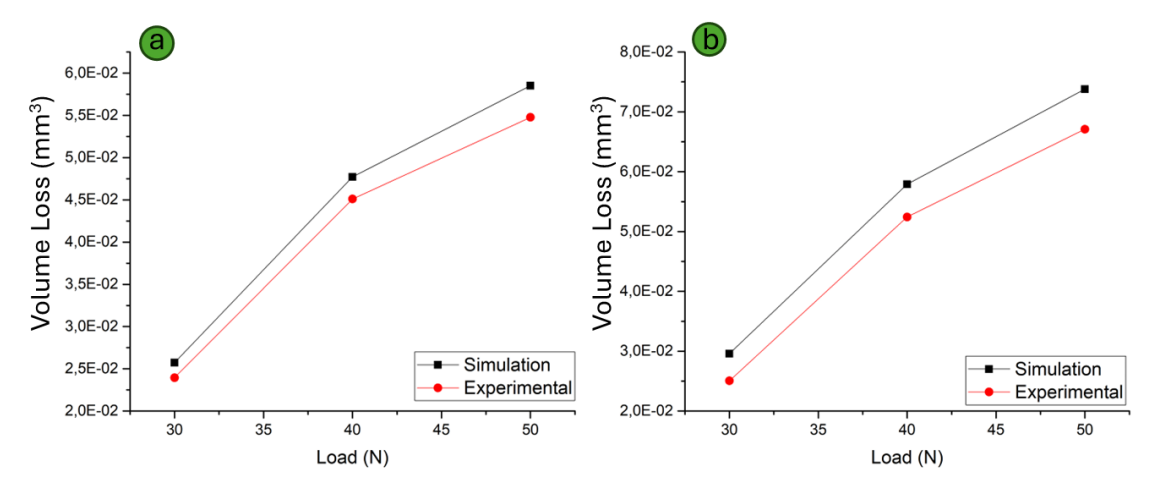


Figure 3. Comparison of volume loss a) 40 mm/s, b) 50 mm/s.

3.3. Evaluation of Friction Coefficients in Wear Test

The friction coefficient values occurring at different loads are presented graphically in Figure 4. The friction coefficient value increased depending on the increase in load. The highest friction coefficient value at 40 mm/s speed was 0.83 and at 50 N load. This value decreased by 26.5% at 40 N load and by 45.78% at 30 N load. There is a 10.76% increase in the average friction coefficient when going from 40 mm/s speed to 50 mm/s speed. The study by Zhang et al. [30] strongly supports these results. The characteristics of the third body formation between the sliding surfaces determine the friction and wear at low loads. They wear particles in the ball and plate samples formed a friction layer by their oxidation. The ball, acting as an abrasive while sliding, caused the friction layer in the wear zone to lift. This restricts the friction layer from extending continuously at higher loads. The results of this study align well with existing literature, indicating consistency with prior research on the wear behaviour of Monel 400 under different conditions. This alignment enhances the reliability of the observed trends and offers additional validation for the current understanding of the material's tribological performance [9–11].

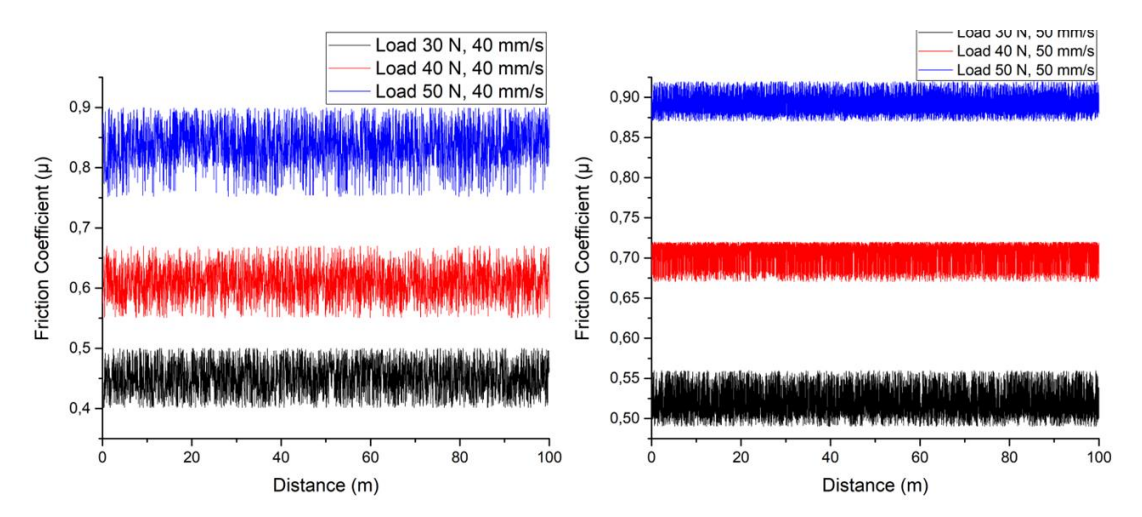


Figure 4. Comparison of friction coefficients in the sliding distance of the ball at different loading conditions (30 N, 40 N and 50 N) and speeds of a) 40 mm/s and b) 50 mm/s.

4. CONCLUSIONS

This research presents novel insights into wear mechanisms by investigating the wear behaviour of Monel 400 across various load and speed conditions through both experimental tests and simulations. In the wear tests, a WC ball was utilised as the abrasive, and the resulting data were analysed in accordance with Archard's wear law principles. The findings indicate that the finite element model utilising the perfect contact method effectively predicts the deformation distribution on the wear surface during dry sliding. The analysis confirmed a significant effect of increasing load and speed conditions on wear amount, revealing that volume loss increased markedly, particularly under high load conditions. This study offers a thorough analysis of the wear resistance of Monel 400 through the integration of experimental and numerical findings. The findings indicate the material's potential for engineering applications that demand high wear resistance. Future research should broaden its scope to include various abrasive materials and environmental factors, thereby enhancing the understanding of wear mechanisms.

REFERENCES

- [1] U. Esgin, D. Özyürek, H. Kaya, An investigation of wear behaviors of different Monel alloys produced by powder metallurgy, in: 2016: p. 020008. https://doi.org/10.1063/1.4945963.
- [2] M. Kukliński, A. Bartkowska, D. Przestacki, G. Kinal, Influence of Microstructure and Chemical Composition on Microhardness and Wear Properties of Laser Borided Monel 400, Materials 13 (2020) 5757. https://doi.org/10.3390/ma13245757.
- [3] E.O. Ezugwu, J. Bonney, Y. Yamane, An overview of the machinability of aeroengine alloys, J Mater Process Technol 134 (2003) 233–253. https://doi.org/10.1016/S0924-0136(02)01042-7.
- [4] R.S. Dutta, Corrosion aspects of Ni–Cr–Fe based and Ni–Cu based steam generator tube materials, Journal of Nuclear Materials 393 (2009) 343–349. https://doi.org/10.1016/j.jnucmat.2009.06.020.
- [5] M. Wiciak-Pikuła, A. Felusiak-Czyryca, P. Twardowski, Tool Wear Prediction Based on Artificial Neural Network during Aluminum Matrix Composite Milling, Sensors 20 (2020) 5798. https://doi.org/10.3390/s20205798.
- [6] M.S. Gul, R. Demirsöz, S. Kabave Kilincarslan, R. Polat, M.H. Cetin, Effect of Impact Angle and Speed, and Weight Abrasive Concentration on AISI 1015 and 304 Steel Exposed to Erosive Wear, J Mater Eng Perform (2024). https://doi.org/10.1007/s11665-023-09117-4.
- [7] F. Ma, Z. Zeng, Y. Gao, Tribocorrosion and the surface repassivation behavior of Monel 400 alloy in artificial seawater, Industrial Lubrication and Tribology 70 (2018) 1331–1340. https://doi.org/10.1108/ILT-09-2017-0266.
- [8] M. Kuklinski, A. Bartkowska, D. Przestacki, Laser Alloying Monel 400 with Amorphous Boron to Obtain Hard Coatings, Materials 12 (2019) 3494. https://doi.org/10.3390/ma12213494.
- [9] C.H. Zhang, N. Yan, Y.X. Hao, C. Wang, X. Bian, S. Zhang, Study on Cavitation Erosion Behavior of Monel Alloys in the Simulated Seawater Solution, Adv Mat Res 631–632 (2013) 40–43. https://doi.org/10.4028/www.scientific.net/AMR.631-632.40.
- [10] M. Mahalingam, R. Varahamoorthi, Investigation on tool wear rate of brass tool during machining of Monel 400 alloy using electric discharge machine, Mater Today Proc 26 (2020) 1213–1220. https://doi.org/10.1016/j.matpr.2020.02.244.
- [11] P. Sudhakar Rao, A. Sinha, S.G. Patil, R. Kant, S.P. Sushma, Machining performance and optimization of process parameters of monel alloy 400 using ECM process, in: Modern Materials and Manufacturing Techniques, CRC Press, Boca Raton, 2024: pp. 288–305. https://doi.org/10.1201/9781032703046-11.
- [12] A. Kumar, M. Nikam, T. Jagadeesha, A.U. Rehman, A.S. Bhongade, T. Shivagond, PMEDM process parameter optimization for machining superalloy MONEL 400, Mater Res Express 12 (2025) 026506. https://doi.org/10.1088/2053-1591/adb0a4.
- [13] Y. Küçük, K.M. Döleker, M.S. Gök, S. Dal, Y. Altınay, A. Erdoğan, Microstructure, hardness and high temperature wear characteristics of boronized Monel 400, Surf Coat Technol 436 (2022) 128277. https://doi.org/10.1016/j.surfcoat.2022.128277.
- [14] M.M. Karaca, S. Polat, İ. Esen, Reciprocating dry sliding wear behaviour of BN@MXene@AA7075 composites, J Compos Mater 58 (2024) 2007–2026. https://doi.org/10.1177/00219983241257665.
- [15] J.F. Archard, Contact and Rubbing of Flat Surfaces, J Appl Phys 24 (1953) 981–988. https://doi.org/10.1063/1.1721448.
- [16] F. Gelana, Wear Analysis Of Overhead Line Contact Wire Using Ansys Workbench Software, (2015).
- [17] J.M. Thompson, A Proposal for the Wear Calculation, Department of Mechanical Engineering, MIT (2007) 45–57.
- [18] J.L. Sullivan, Boundary lubrication and oxidational wear, J Phys D Appl Phys 19 (1986) 1999–2011. https://doi.org/10.1088/0022-3727/19/10/025.
- [19] J.B. Krolczyk, R.W. Maruda, G.M. Krolczyk, S. Wojciechowski, M.K. Gupta, M.E. Korkmaz, Investigations on surface induced tribological characteristics in MQCL assisted machining of duplex stainless steel, Journal of Materials Research and Technology 18 (2022) 2754–2769. https://doi.org/10.1016/J.JMRT.2022.03.167.

- [20] M. Danish, M.K. Gupta, S. Rubaiee, A. Ahmed, M.E. Korkmaz, Influence of hybrid Cryo-MQL lubri-cooling strategy on the machining and tribological characteristics of Inconel 718, Tribol Int 163 (2021) 107178. https://doi.org/10.1016/j.triboint.2021.107178.
- [21] G. Uslu, M.E. Korkmaz, R.H.R. Elkilani, M.K. Gupta, G. Vashishtha, Investigation of Tribological Properties of Inconel 601 under Environmentally Friendly MQL and Nano-Fluid MQL with Pack Boronizing, Lubricants 12 (2024) 353. https://doi.org/10.3390/lubricants12100353.
- [22] M.T. Özdemir, R. Demirsöz, R. Polat, Enhancing wear resistance of inconel 601 through pack alumunizing coating and advanced lubrication environments, Discov Mater 5 (2025) 27. https://doi.org/10.1007/s43939-025-00205-x.
- [23] M. Buğday, M. Karalı, Ş. Talaş, Wear performance of GGG60 ductile iron rollers coated with WC-Co by electro spark deposition, Revista de Metalurgia 59 (2023) e249. https://doi.org/10.3989/revmetalm.249.
- [24] M. Buğday, M. Karalı, Ş. Talaş, Investigation on Characterization of GGG 60 Coated with WC/Co by ESD Technique, Protection of Metals and Physical Chemistry of Surfaces 59 (2023) 1260–1266. https://doi.org/10.1134/S2070205123701125.
- [25] H.E.L. Etri, A.K. Singla, M.T. Özdemir, M.E. Korkmaz, R. Demirsöz, M.K. Gupta, J.B. Krolczyk, N.S. Ross, Wear performance of Ti-6Al-4 V titanium alloy through nano-doped lubricants, Archives of Civil and Mechanical Engineering 23 (2023) 147. https://doi.org/10.1007/s43452-023-00685-9.
- [26] R. Demirsöz, M.E. Korkmaz, M.K. Gupta, A novel use of hybrid Cryo-MQL system in improving the tribological characteristics of additively manufactured 316 stainless steel against 100 Cr6 alloy, Tribol Int 173 (2022) 107613. https://doi.org/10.1016/j.triboint.2022.107613.
- [27] W.G. Liang, Z.S. Zhang, L. Luo, Rolling friction performance analysis of swash-plate engine in underwater vehicle, Applied Mechanics and Materials 80 (2011) 855–859.
- [28] O. Çakır, R. Demirsöz, M.T. Özdemir, M.E. Korkmaz, M.K. Gupta, M. Günay, N.S. Ross, A. Nag, Investigating the erosive wear characteristics of AISI 420 martensitic stainless steel after surface hardening by boriding, Journal of Materials Research and Technology 33 (2024) 2292–2302. https://doi.org/10.1016/j.jmrt.2024.09.208.
- [29] D. Odabas, Effects of Load and Speed on Wear Rate of Abrasive Wear for 2014 Al Alloy, IOP Conf Ser Mater Sci Eng 295 (2018) 012008. https://doi.org/10.1088/1757-899X/295/1/012008.
- [30] M. Zhang, S. Xu, J. Mo, Z. Xiang, Z. Zhou, Effect of uneven wear on the stability of friction braking system in high-speed train, Eng Fail Anal 158 (2024) 108009.